6ICEGE 6th International Conference on Earthquake Geotechnical Engineering
1-4 November 2015
Christchurch, New Zealand

Numerical Analyses of the Performance of Seismically Isolating Buried Barriers

A. Flora[1], E. Bilotta[2], F. Foria[3], V. Nappa[4]

ABSTRACT

This paper focuses on an unusual kind of ground improvement, introduced as a means to tackle seismic risk. The idea is that a continuous soft layer designed with a proper geometry, with dynamic impedance much smaller than that of the surrounding soil, will filter and reflect most of the incoming seismic energy. The paper presents the results of some 2D parametric numerical analyses aimed to check the seismic performance of this innovative approach. Simplified dynamic inputs (Ricker wavelets, having only one largely predominant frequency) were adopted to better understand the effect of signal frequency. The analyses show that the effectiveness of the soft grouted isolating barrier depends on soil and grouting geometrical, physical and mechanical properties, as well as on the frequency content of the seismic input.

Introduction

The propagation of shear waves in a layered ground depends on the dynamic impedances η (defined as $\eta=\rho \cdot V_S$, where ρ is the material density and V_S the velocity of shear waves) of the single layers via the dynamic impedance ratio α, defined as the ratio $\alpha=\eta_1/\eta_2$ between the dynamic impedance of the layer crossed by the incident wave and that of the adjacent layer crossed by the refracted wave. It is then well known that the properties of the uppermost layers of the ground have an extremely relevant effect on the characteristics of the incoming seismic motion. The idea of artificially modifying them with the aim of reducing in a controlled way the seismic energy at ground level is therefore appealing, with the final goal to protect existing buildings. Ground improvement techniques can be used to this aim. The choice of the best grout properties should be made considering that high frequency components result into large structural loads on massive squat structures (high natural structural frequency), and low frequency components may be critical for tall and flexible structures (low natural structural frequency). The design of a successful grouting intervention of such a kind is not trivial at all, and experimental and numerical tests are needed to get an insight on the behavior of soft grouted barriers. Some authors have recently given some contributions: following the idea of Kirtas and Pitilakis (2009), in particular, Lombardi & Flora (2014) analyzed the effectiveness of soft barriers made with a continuous, thin layer of grouted material, mostly considering the case of a rectangular caisson. A possible technological solution to obtain soft grouted soils is discussed by Flora et al. (2015a). This paper will concentrate on the case of a V shaped soft barrier, that seems more feasible than the rectangular one from a technological point of view (for instance, via inclined partially overlapped series of drillings), presenting the results of some 2D FE analyses.

[1] Associate Professor, University of Napoli Federico II, Naples, Italy, alessandro.flora@unina.it
[2] Assistant Professor, University of Napoli Federico II, Naples, Italy, emilio.bilotta@unina.it
[3] MSc student, University of Napoli Federico II, Naples, Italy, foria.federico@gmail.com
[4] PhD student, University of Napoli Federico II, Naples, Italy, valeria.nappa@unina.it

Parametric Numerical Analyses

FEM Models

2D finite element analyses were carried out by using the numerical code Plaxis (Brinkgreve et al., 2011), modelling the geometric layout of the V shaped soft barrier shown in Figure 1a with the mesh shown in Figure 1b. The mesh bottom is assumed to be rigid and reflective, at a depth z=30 m.

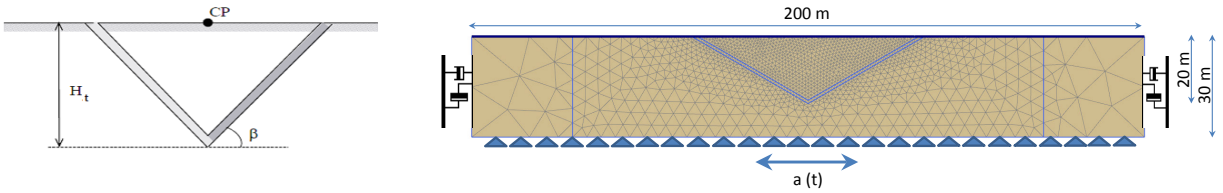

(a) (b)

Figure 1. Geometrical layout of the isolating system (a), FEA mesh (b).

The soil is considered to be a sand, and has been characterized by a constitutive model implemented in the Plaxis code, named Hardening Soil with small strain overlay, that accounts for strain hardening plasticity and small-strain behavior of soils (Schanz et al., 1999; Benz et al., 2009). The model is also able to catch the hysteretic behavior of sand and the associated hysteretic damping in unloading reloading cycles. Both stiffness decay and hysteretic damping are crucial in the prediction of the stress-strain behavior of soil under cycling loads, as in the case of shaking due to earthquakes.

The properties of the sandy ground have been calibrated on the basis of the available characterization of Leighton Buzzard sand (LB) fraction E (Lanzano et al., 2015), assuming three different values of initial stiffness (Table 1).

The initial soil damping, corresponding to very low strain levels (for which soil behavior is not hysteretic), is D_0=1%, and it has been introduced in the analyses through the common Rayleigh approach. Out of such a small strain linear range, the hysteretic damping (D-D_0) increases with strain to a maximum value reached for a shear strain of 0.1%. Fig. 2 reports the normalized shear stiffness G/G_0 and damping ratio D-D_0 for the considered sand.

Table 1. Hardening Soil small strain model parameters for the sandy ground (p_{ref}=100kPa).

	γ (kN/m^3)	$E_{50,ref}$ (MPa)	$E_{oed,ref}$ (MPa)	$E_{ur,ref}$ (MPa)	$G_{0,ref}$ (MPa)	ν_{ur}	m	$\gamma_{0.7}$	$\gamma_{cut-off}$	ϕ_{pk} (°)	ψ_{pk} (°)	c' (kPa)
S1	14.5	9.3	10.2	31.1	36.3	0.2	0.4	$5.8 \cdot 10^{-4}$	$10.1 \cdot 10^{-4}$	38.6	8.2	0.01
S2	15.0	18.6	20.5	62.2	72.7							
S3	15.5	18.6	20.5	124.3	145.4							

Table 2. Parameters for the grouted material

$V_{s,b}$ (m/s)	ρ_b (kg/m^3)	G_b (MPa)	ν_b	ϕ_b (°)	ψ_b (°)
10; 20	1000	0.1; 0.4	0.45	5; 15	0

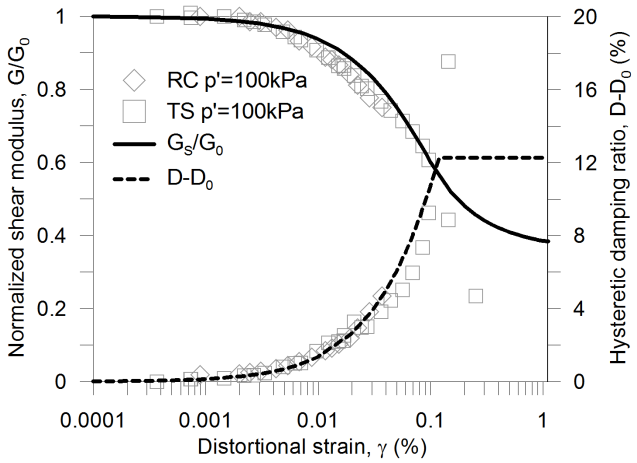

Figure 2. Normalized shear stiffness and damping ratio of sand (after Lanzano et al., 2015).

Table 3. Summary of the FEA models adopted in the calculations.

Description	Dynamic impedance ratio, $\alpha=\eta_s/\eta_b$	Friction angle of grouted soil, ϕ_b (°)
No treatment in sand S1	-	-
Sand S1 with soft barrier	12	5
		15
	23	5
		15
No treatment in sand S2	-	-
Sand S2 with soft barrier	17	5
		15
	33	5
		15
No treatment in sand S3	-	-
Sand S3 with soft barrier	23	5
		15
	47	5
		15

The V-shaped soft barrier has H_b= 20 m and β=30° (Figure 1.a), and a thickness of 1 m.

The material of the barrier is modeled as elastic – perfectly plastic. Its properties will be identified by a subscript "b" (for "barrier") and are: shear wave velocity $V_{s,b}$, density ρ_b, shear stiffness G_b, Poisson ratio ν_b, friction angle ϕ_b, dilation angle ψ_b. They have been assigned on the basis of the experimental results published by Flora et al. (2015b) on a polymeric soft grout, and are reported in Table 2. In order to consider different kinds of soft grout, or better different percentages of grout and soil, two values of $V_{s,b}$ and ϕ_b were considered.

An overview of the analyzed models is shown in Table 3.

Input Signals

Synthetic seismograms called Ricker wavelets (Ryan, 1994) have been used to generate the stress histories to be applied at the bottom of the mesh. The normalized values of acceleration, displacement and velocity (a), and the amplitude Fourier spectrum of acceleration (b) are shown in Figure 3 for one of the used Ricker wavelet (peak frequency of 1Hz, in terms of displacements). For each geometrical scheme, the calculation has been performed for different values of the characteristic frequency: 0.5Hz, 1Hz, 2Hz, 5Hz. The amplitude of the wavelet at the base of the model is in all cases a_{max}=0.5g. Such a large peak acceleration has been chosen to induce large strains in the soil and therefore both soil yielding and shear stiffness decay with associated large damping. Such a condition is interesting to check the seismic performance of the V-shaped barrier, as it largely reduces the operative impedance ratio between the soil impedance η_s and the barrier impedance η_b.

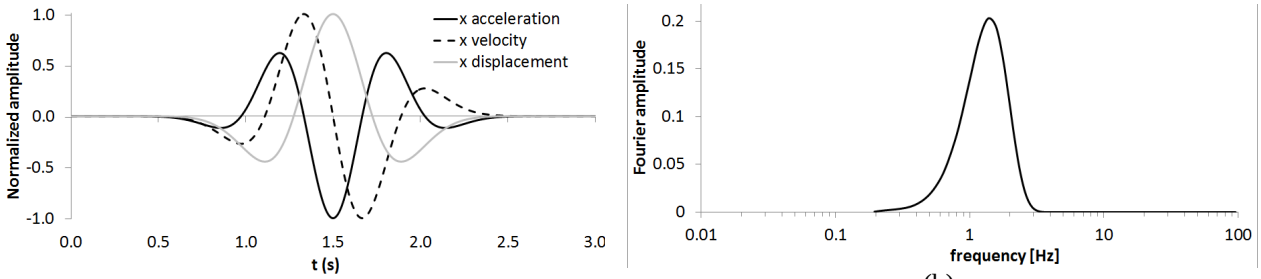

(a) (b)

Figure 3. Normalized time histories (a) and Fourier amplitude of acceleration (b) of a Ricker wavelet (f=1 Hz in terms of displacements)

Calculation Results

As an example of the effect of the ground treatment, the calculated Fourier spectrum at the control point CP (see Figure 1a) in the case of S3 sand without soft barrier is compared in Figure 4a with the corresponding spectrum for the case of the same sand with a soft barrier having $V_{s,b}$=20 m/s (α=23), for the input wavelet with nominal frequency of 2 Hz. In this case, the soft barrier has the beneficial effect of reducing the Fourier amplitude for almost all the frequencies, being most beneficial in this case for the range 2-5 Hz.

In Figure 4b the same results are plotted in terms of attenuation ratio, defined as the ratio between the Fourier amplitude at the control point with the isolation system and the corresponding one without any treatment. When the calculated attenuation ratio is below 1, the soft shield reduces the amplitude of the corresponding harmonic in the propagated signal. Despite some unavoidable scatter, the figure clearly shows the positive effect of the soft barrier.
In order to get a better insight on the influence of the several factors affecting the effectiveness of the ground treatment, the results of the whole set of analyses have been summarized using two popular synthetic parameters: the first is the Arias Intensity (Arias, 1970):

$$I_a = \frac{\pi}{2g}\int_0^{\infty}(a(t))^2 dt \qquad (1)$$

which accounts for the energy of the signal in the control point; the second is the Housner Response Spectrum Intensity (Housner, 1959) defined as:

$$HI = \int_{0.1s}^{2.5s} S_v(\xi = 0.05, T)dT \quad (2)$$

which is able to summarize the signal structural damage potential in a wide range of structural periods ($0.1 \leq T \leq 2.5$) for a given value of structural damping (ξ=0.05 in this case).

The ratio between the Arias Intensity at point CP with the soft barrier (AI_{SOIL+V}) and without it (AI_{SOIL}) thus represents a convenient quantification of the effectiveness of the isolating intervention: values lower than 1 indicate a beneficial effect of the soft barrier, while values larger than 1 imply detrimental effects. Figure 5 summarizes the results of all the analyses carried out with ϕ_b=5° in terms of the ratio AI_{SOIL+V}/AI_{SOIL} versus the nominal frequency of the input wavelet f_i. The figure clearly shows that the barrier reduces the incoming energy in all the analyzed cases, with an effectiveness that increases with f_i and with α. For the two cases having the largest values of the dynamic impedance ratio α (33 and 47), the Arias Intensity with the soft barrier reduces to less than 0.1 of the original one, for f_i equal or larger than 1 Hz.

Similar information can be obtained by looking at the results in terms of the ratios between the Housner Intensity with the barrier (HI_{SOIL+V}) and the one without (HI_{SOIL}). In Figure 6, such ratios are plotted as a function of the impedance ratio α for the two nominal frequencies of 1 Hz and 5 Hz of the input wavelet. This figure confirms the beneficial effect of the barrier because in all cases the ratios HI_{SOIL+V}/HI_{SOIL} are lower than 1, but also confirms that the soft barrier is most effective for higher input frequencies f_i and impedance ratios α. The figure also shows that the influence of the friction angle ϕ_b of the material composing the soft barrier is negligible for f_i=5 Hz, while for f_i=1 the barrier is more effective for the lower value of ϕ_b.

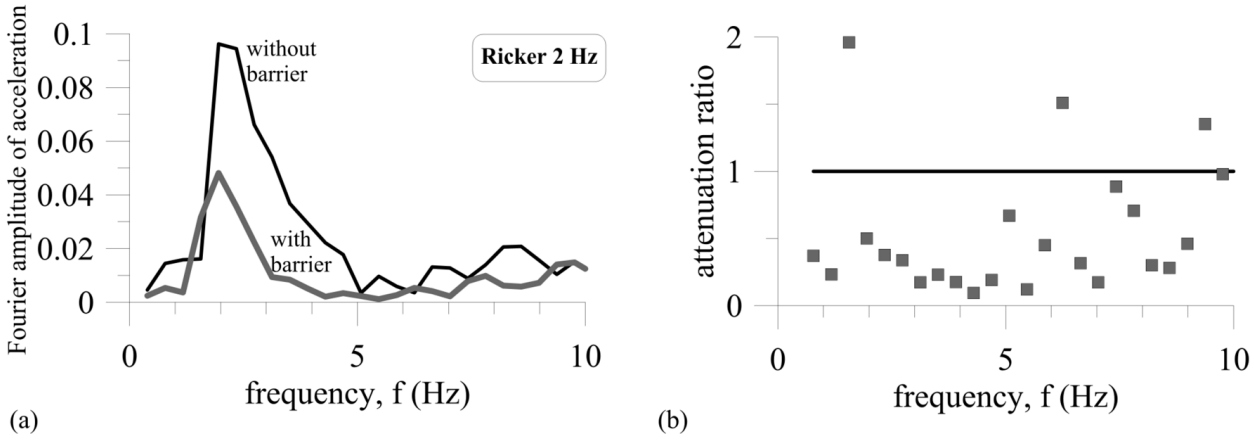

Figure 4. Fourier spectra of acceleration amplitude calculated at the control point (CP) (input frequency f_i=2 Hz), with and without soft barrier (a) and corresponding attenuation ratio (b), for the case of sand S3, $V_{s,b}$=20 m/s and ϕ_b=15°.

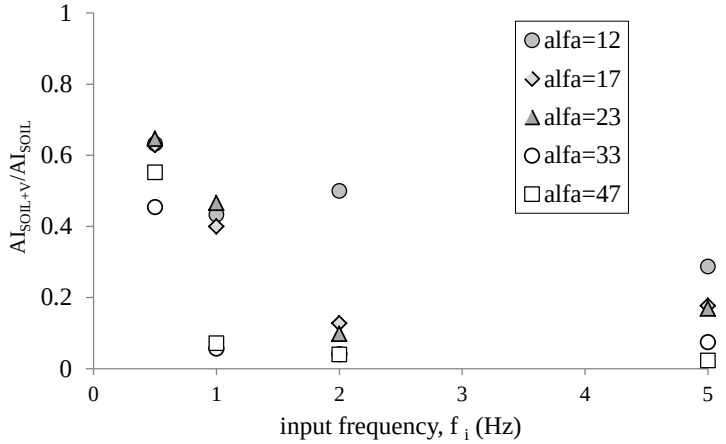

Figure 5. Attenuation ratio at control point CP in terms of Arias Intensity, for all the analyses having ϕ_b=5°.

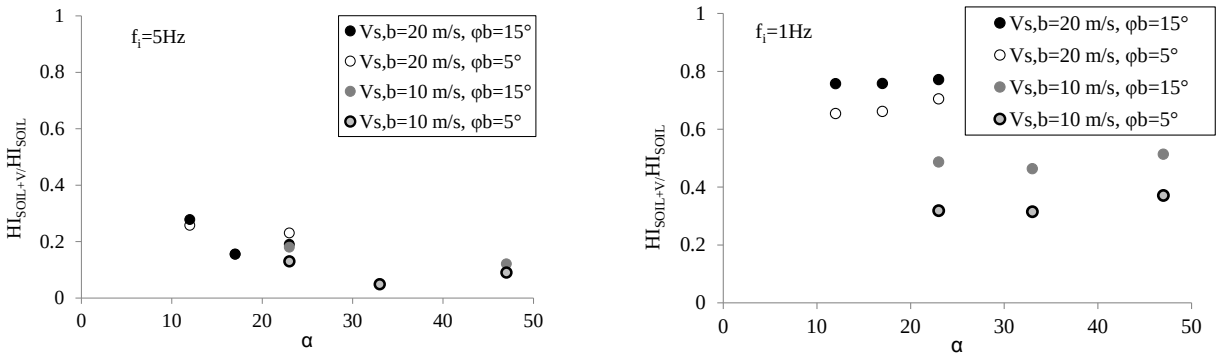

Figure 6. Attenuation ratio in terms of Housner Intensity: a) f=5 Hz, b) f=1 Hz.

In order to gather more general information from the results, the nominal input frequency f_i should be properly taken into account as a relevant parameter. In this case, considering the ratio HI_{SOIL+V}/HI_{SOIL} as the indicator of the barrier isolating effectiveness, such a thing has been done in a dimensionless way considering the following formal relation:

$$\frac{HI_{SOIL+V}}{HI_{SOIL}} = f\left(\alpha \cdot \frac{f_i}{f_s}\right) \tag{3}$$

where f_s is the first natural frequency of the ground layer (the natural frequencies of the three sandy layers are: $f_s(S1)$=1.3 Hz, $f_s(S2)$=1.8 Hz, $f_s(S3)$=2.6 Hz).

All the results of the parametric analyses have been then analyzed considering the formal relation (3). Figure 7 shows that the dimensionless group $\alpha \cdot f_i/f_s$ is a relevant one, as all the considered data (from all the analyses with ϕ_b=15°) seem to follow a unique trend. This has been identified with a Pearson type IV distribution with ±10% confidence range. Even though there is some

scatter in the results, it is clear that the effectiveness of the barrier should be calibrated considering the frequencies of the seismic input that are expected to have the highest energy content. The higher such frequencies, the lower the need to have very soft barriers.

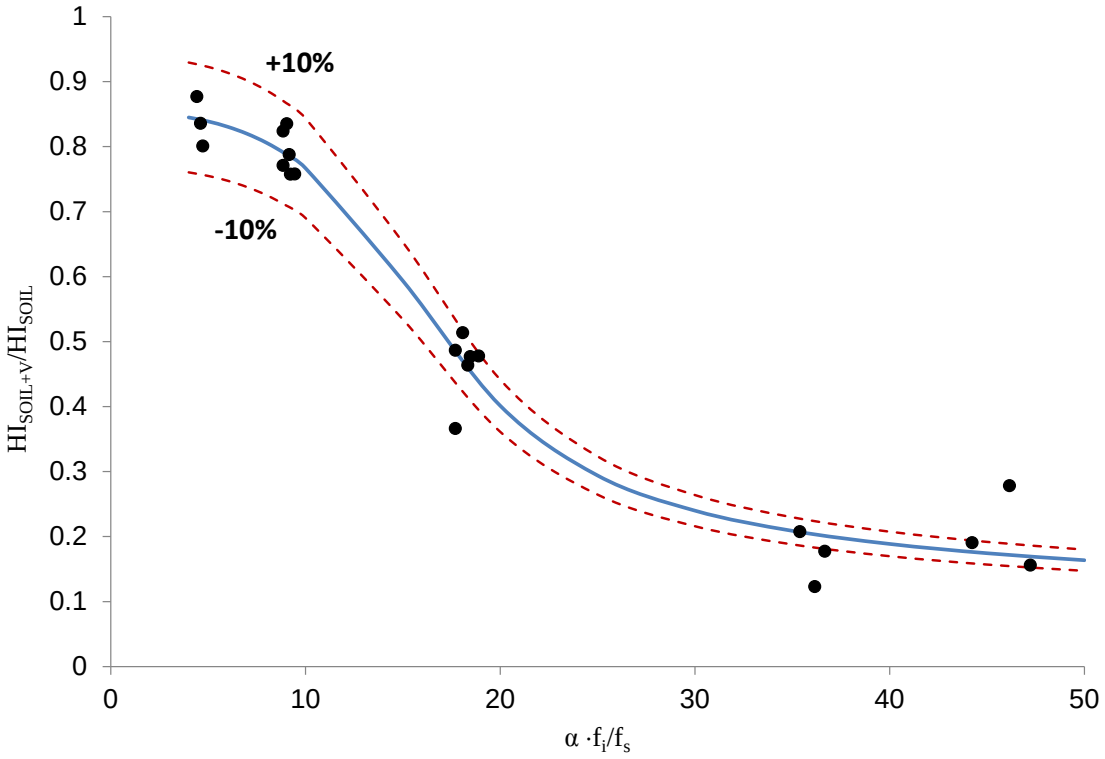

Figure 7. Attenuation ratio in terms of Housner Intensity versus the dimensionless group $\alpha \cdot f_i/f_s$ for the analyses with $\phi_b=15°$.

Conclusions

Ground treatment underneath existing buildings is a possible measure to protect them against earthquakes. At this aim, V-shaped barriers can be created with inclined and partially overlapped drillings. The numerical parametric analyses reported in the paper show that such barriers can be extremely effective in reducing both the energy and the destructive potential of the dynamic motion inside the bounded volume of soil.

The barriers are most effective when the dynamic impedance ratio α between the natural soil and the material of the barrier is large, and when the seismic input has higher dominant frequencies. Since such frequencies are most dangerous for squat structures, soft barriers seem best suited to protect such kind of buildings.

As the parameters to be considered for the assessment of the seismic isolating effectiveness of the soft barrier are numerous, in the paper a first attempt to group some of them in a dimensionless factor is reported. In such a way, all the results can be looked at in a consistent way, as reported in Figure 7. The parametric analysis is ongoing to confirm these first promising results.

References

Arias A. A measure of earthquake intensity. In R.J. Hansen, ed. *Seismic Design for Nuclear Power Plants*, MIT Press, Cambridge, Massachusetts: 438-483. 1970.

Benz T, Vermeer PA, Schwab R. A small-strain overlay model. *International Journal of Numerical and Analytical Methods in Geomechanics*, 2009; **33**(1): 25 - 44.

Brinkgreve RBJ, Swolfs WM, Engine E. PLAXIS user's manual, PLAXIS bv, the Netherlands. 2011.

Flora A, Bilotta E, Foria F, Nappa V. Soft deep mixing for the mitigation of seismic risk. *Deep Mixing conference 2015*, San Francisco. 2015.

Flora A, Bilotta E, Lirer S, Nappa V. Soft soil-polymer mixtures for seismic isolation. *6th International Symposium on Deformation Characteristics of Geomaterials*, Buenos Aires. 2015.

Housner GW. Behavior of structures during earthquakes. *Journal of the Engineering Mechanics Division*, ASCE, 1959; **85**(EM14): 109-129.

Kirtas E, Pitilakis K. Subsoil Interventions Effect on Structural Seismic Response. Part II: Parametric Investigation. *Journal of Earthquake Engineering*, 2009; 13(3): 328-344.

Lanzano G, Visone C, Bilotta E, Santucci de Magistris F. Experimental assessment of the stress-strain behaviour of Leighton Buzzard Sand for the calibration of a constitutive model. Submitted. 2015.

Lombardi D., Flora A. Numerical analyses of the effectiveness of soft barriers into the soil for the mitigation of seismic risk. Submitted to *Soil Dynamics and Earthquake Engineering*. 2014.

Ryan H. Ricker, Ormsby, Klauder, Butterworth- A choice of wavelets. *CSEG Recorder*, 1994; **19**(7): 8-9.

Schanz T, Vermeer PA, Bonnier PG. The hardening soil model: formulation and verification. In *Beyond 2000 in computation geotechnics* (ed. R. B. J. Brinkgreve): 281–290. Rotterdam: Balkema. 1999.